Design and Characterization of a Novel Hybrid Actuator Using Shape Memory Alloy and DC Micromotor for Minimally Invasive Surgery Applications

Venkata Raghavaiah Chowdhary Kode and M. Cenk Çavuşoğlu, *Senior Member, IEEE*

***Abstract*—The end-effectors in the state-of-the-art robotic tools for minimally invasive surgery (MIS) are actuated by actuator packs located outside the patient's body, with the power transmitted from the actuator pack to the end-effector by means of sliding link or tendon-driven mechanisms. This method of power transmission limits the number of degrees-of-freedom (DOFs) in these systems, as the design of a spherical wrist gets complicated. The design of the spherical wrists can be simplified, and the number of DOFs increased, if local actuation is used for the end-effector. However, there are no suitable actuation systems available in the literature. In this paper, a novel design idea for developing a millimeter-scale actuator is presented for locally actuating the end-effector (5-mm-diameter laparoscopic needle driver) for a robot performing MIS. This actuator is designed by combining a dc micromotor and a shape memory alloy actuator in series. The designed actuator is 5.14 mm in diameter (including casing) and 40 mm in length, and is used to actuate a 20-mm-long needle driver assembly, while generating a force of 24 N, resulting in a gripping force of 8 N. The total stroke length of the actuator is 1 mm, which results in a 45° opening of the needle driver jaw with a gap of 8 mm in between the jaws.**

***Index Terms*—Medical robotics, millimeter-scale actuators, minimally invasive surgery (MIS), shape memory alloy (SMA) actuator.**

I. Introduction

MEDICAL robotics for surgery is a new and promising field for innovation in robotics, focusing on the development of new tools for enhancing the capabilities of surgeons. In this paper, the design and characterization of a hybrid millimeter-scale actuator for locally actuating the end-effector, a 5-mm-diameter laparoscopic needle driver, of a robotic minimally invasive surgery (MIS) system are discussed. This hybrid actuator can be used to improve the number of degrees-of-freedom (DOFs) for robotic tools used in performing MIS.

Manuscript received October 20, 2006; revised April 7, 2007. Recommended by Technical Editor J. P. Desai. This work was supported in part by the National Science Foundation under Grant CISE IIS-0222743, Grant EIA-0329811, and Grant CNS-0423253, and in part by the U.S. Department of Commerce under Grant TOP-39-60-04003. Parts of this paper were presented at the 2005 IEEE International Conference on Mechatronics and Automation (ICMA 2005), Niagara Falls, ON, Canada, July 29–August 1.

V. R. C. Kode is with Visicon Inspection Technologies, Napa, CA 94558 USA (e-mail: venkata.kode@case.edu).

M. C. Çavuşoğlu is with the Department of Electrical Engineering and Computer Science, Case Western Reserve University, Cleveland, OH 44106 USA (e-mail: cavusoglu@case.edu).

Digital Object Identifier 10.1109/TMECH.2007.901940

Laparoscopic surgery is a revolutionary surgical technique [1] that is minimally invasive. In laparoscopic surgery, the operation is performed with instruments inserted through small incisions (less than 10 mm in diameter) rather than by making a large incision to expose the operation site. The main advantage of this technique is the reduced trauma to the healthy tissue, which is the leading cause of postoperative pain and long hospital stay of the patient. The hospital stay and rest periods, and the resulting procedure's cost, are significantly reduced with MIS, at the expense of more difficult techniques currently performed by surgeons. Adoption of laparoscopic techniques has been slower in more complex procedures, largely because of the greater difficulty due to the surgeon's reduced dexterity and perception of the operation.

There are two commercially available telemanipulation systems that are currently in use for minimally invasive cardiac surgery: the da Vinci Robotic System (Intuitive Surgical, Inc., Sunnyvale, CA) and the Zeus Robotic System[1] (formerly Computer Motion, Inc., now part of Intuitive Surgical). In order to generate high gripping forces at the end-effectors while maintaining small instrument sizes, the power transmission mechanisms in these systems are designed in such a way that the motors are placed outside the human body. The da Vinci Robotic system uses a tendon-driven mechanism, and the Zeus Robotic system uses a serial linkage mechanism for transmitting the power from the motors to the end-effector. The da Vinci system has an instrument diameter of 8 mm, and includes a robotic wrist at the end of the instruments that provide articulated motions with 6 DOFs[2] of movement inside the chest cavity, in contrast to the Zeus system that has an instrument diameter of 5 mm, but lacks a fully articulated (i.e., 2 DOFs) wrist allowing only 5 DOFs inside the chest cavity. The Zeus system, on the other hand, requires a significantly smaller incision to be made on the body over the da Vinci system. More recently, 5-mm-diameter instruments with full 6 DOFs have been available for the da Vinci system. However, these instruments use a nonspherical wrist, which result in reduced dexterity. The same general relationship between the number of DOFs of a surgical manipulator and its tool shaft diameter holds for the other robotic laparoscopic surgery systems reported in the literature as well (for a recent review, refer to [2]).

[1]Zeus system is no longer commercially available.

[2]Not including the end-effector action in the DOF counts.

If the robot has a multi-DOF wrist, then the number of DOFs for the end-effector can be increased, which allows the surgeon to perform the surgery with more dexterity. A conflicting objective is to reduce the diameter of the multi-DOF robotic surgical instruments to allow their use in variety of applications, including minimally invasive pediatric, neonatal, and fetal surgery. Due to the present actuator technologies available for the end-effector and power transmission for orienting the end-effector, it is difficult to design a multi-DOF wrist for orienting the end-effector of a 5-mm-diameter robotic instrument for MIS. If we can integrate a local actuating system with the end-effector itself, this would simplify the wrist design, facilitating the construction of wrists with higher DOFs at smaller diameters, as we can eliminate the transmission of the mechanical power through the wrist to the end-effector. Developing a device for local actuation is, therefore, an important enabling technology for designing new tools for MIS.

There are a number of earlier works in the literature that focused on the design of robotic end-effectors with integrated actuators, including compliant and flexure-based grippers [3], [4], instruments with embedded sensors [5], [6], and end-effectors employing SMA and other microactuators [7]–[9]. However, none of these system designs satisfies the requirements of this application.

In this paper, the design of a novel hybrid actuator driven by a miniature brushless dc motor and shape memory alloy (SMA) actuator is presented to overcome the present limitations of current MIS tools. The developed hybrid actuator is used to actuate a 5-mm-diameter endoscopic needle driver (adapted from a manual endoscopic needle driver manufactured by Ethicon Endo-Surgery, Inc.) that will be used as an end-effector in a robotic telesurgical system for minimally invasive cardiothoracic surgery. The designed actuator is 5.14 mm in diameter (including the casing) and 40 mm in length, and is used to actuate 20-mm-long needle driver assembly, while generating a force of 24 N, resulting in a gripping force of 8 N. The total stroke length of the actuator is 1 mm, which results in a 45° opening of the needle driver jaw with a gap of 8 mm in between the jaws.

The rest of the paper is organized as follows. The design requirements and a review of alternative actuation technologies is presented in Section II, followed by the presentation of the design principles of the proposed hybrid actuator in Section III. The method used to determine the SMA actuator force–displacement characteristics is presented in Section IV. The design and experimental evaluation results of the first- and second-generation hybrid actuator prototypes are discussed in Section V and VI, respectively, followed by concluding remarks in Section VII.

II. Design Considerations

A. Design Requirements

The goal of the design is to develop a millimeter-scale actuator that can be used locally to actuate laparoscopic needle driver jaws, thereby facilitating the development of a multi-DOF wrist and developing a robot with more DOFs for performing MIS.

TABLE I
Design Requirements for the Actuator

Parameter	Value
Dimension: overall diameter	5mm (maximum)
Gripping force	5N (minimum)
Stroke length	1mm (minimum)
Gripper closing time	2 seconds (maximum)

The requirements for the millimeter-scale actuator used during the design are summarized in Table I. The actuator should be 5 mm in diameter so that it can fit through the 5-mm trocars. The gripping force needs to be sufficiently large to hold the needle while suturing. The minimum gripping force requirement was determined based on simple experiments done with the specific needle driver used as the end-effector. This value is consistent with the values used in [10], and in [11], for the Silver Falcon system. The stroke length of the actuator is also determined from the specific needle driver used as the end-effector so as to result in a 45° opening of the needle driver jaw.

The wrist-to-gripper length of the manipulator has implications in terms of the dexterity of the manipulator, where a shorter wrist-to-gripper length typically results in smaller joint velocities during surgical manipulation. Therefore, the length of the end-effector should be as short as possible so that it can be attached to a spherical wrist of a robot performing MIS. However, in this study, we chose to focus on the diameter of the actuator rather than on the overall length, as there are types of minimally invasive surgical operations where the instrument diameter is critical, and there are no existing designs that can satisfy their requirements, as discussed in Section I. The specified minimum cycle time for the gripper actuation is chosen specifically for needle driving applications where the needle is held for long durations once it is properly grabbed, in contrast to manipulations, such as dissection, which requires much more end-effector openings–closings.

B. Comparison of Various Design Alternatives

Several different microactuator technologies were considered to achieve the design requirements [12]–[15]. From the comparison chart shown in Table II, it can be seen that the amount of force generated per unit volume is high for piezoelectric and SMA actuators. But the amount of stroke produced by piezoelectric actuators is significantly lower than that produced by the other alternatives. One method used to improve the stroke length of piezoelectric actuators is to construct an inchworm mechanism. A 7-mm-diameter actuator is designed in [16] by using piezoelectric crystals to operate as an inchworm actuator to drive the laparoscopic needle driver. This actuator can only be inserted through 8-mm or larger diameter trocars as compared to the 5-mm trocar in our present design. A major issue with piezoelectric inchworm actuators is extremely small tolerances required during manufacturing for the actuator to operate properly.

SMA wires were used in the design of different actuators [17]–[19] for many applications. Silent actuation is a positive

TABLE II
COMPARISON OF DIFFERENT ACTUATION TECHNOLOGIES (ADAPTED FROM KORNBLUH *et al.* [20])

Actuator type	Strain (Max, %)	Pressure (Max, MPa)	Efficiency (Max, %)	Relative Speed (Full Cycle)	Power Density
Electromagnetic (Voice Coil)	50	0.10	>90	Fast	High
Piezoelectric					
Ceramic (PZT)	0.2	110	>90	Fast	High
Single Crystal (PZN-PT)	1.7	131	>90	Fast	
Polymer (PVDF)	0.1	4.8	n/a	Fast	
Electrostatic Devices (Integrated force array)	50	0.03	>90	Fast	Low
Shape Memory Polymer	100	4	<10	Slow	Medium
Thermal (expansion)	1	78	<10	Slow	Medium
Magnetostrictive (Terfenol- D. Etrema Products)	0.2	70	60	Fast	Very High

attribute that allows the use of SMA in medical applications. But, the major problem with the use of an SMA actuator is its low cycle speed and low stroke length. Its efficiency is low, requiring a large power to actuate. However, in the present application, power is not an issue.

Another alternative actuator technology choice is dc micromotors, which have a good speed and large stroke, but a low output torque. With the advances in miniaturization and the production of miniature brushless dc motors with microgearbox, the feasibility of using dc motors in miniature applications has increased. Micro dc motors have been investigated in [21]–[23] as a linear actuator in the design of miniature medical devices.

No single actuator technology can be employed to satisfy the requirements specified in Table I. Each of the actuator types discussed earlier (and presented in Table II) has shortcomings in some of the aspects.

Both the SMA and dc micromotor have positive attributes and drawbacks for designing the millimeter-scale actuator. In this paper, we propose a design solution that combines SMA and dc micromotors in a hybrid fashion in complimentary roles harvesting the positive attributes and overcoming the drawbacks of both these actuator technologies.

III. DESIGN PRINCIPLE OF THE HYBRID ACTUATOR

The proposed novel hybrid actuator design consists of two stages: a dc micromotor stage and an SMA actuator stage. The two stages of the hybrid actuator are connected in series, and it works as a two-phase actuator. The dc micromotor stage is composed of a dc micromotor and a leadscrew connected to its rotor shaft with a rotational bearing. The bearing is for protecting the dc micromotor from the large axial forces generated by the SMA actuator stage, and the lead-screw and nut assembly is for converting the rotational motion of the motor to linear motion. The SMA actuator stage is composed of several SMA wires

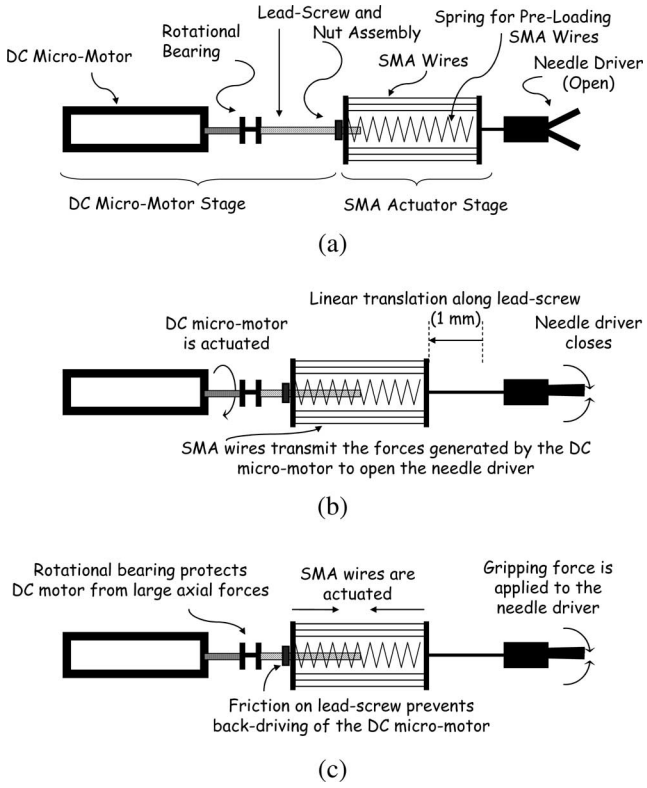

Fig. 1 Hybrid actuator operates in two phases during needle grasping action. (a) Initial configuration and parts of the hybrid actuator. (b) In the first phase of actuation, the dc micromotor is actuated to close the needle driver jaws. (c) In the second phase of actuation, SMA actuator is actuated to generate the force required to hold the needle. (The figures are not to scale.)

and a preloading spring connected in a mechanically parallel fashion, and is connected to the nut of the lead-screw and nut assembly of the dc micromotor stage.

Each of the two stages are used in roles that harvest the corresponding actuator technology's advantages while avoiding the shortcomings. The dc micromotor stage is used for opening and closing action of the gripper jaws, as this action requires large strokes (in the order of 1 mm) but significantly smaller forces (in the order of 1 N). The SMA actuator stage is used for gripping and holding the needle, as this action requires substantial forces (about 15 N for gripping force of 5 N) but relatively short strokes (only enough to handle the structural deformations). Both the SMA actuator and the dc motor are actuated in closing the needle driver jaws to hold the suture needle, and only the dc motor is actuated in opening the needle driver jaws.

A. Closing the Needle Driver Jaws

The hybrid actuator operates in two phases during needle grasping action. In the first phase of actuation, as shown in Fig. 1(b), the dc motor rotates in counterclockwise direction, and moves the needle driver jaws from the open position to the closed position. In the second phase of the actuation [Fig. 1(c)], when the jaws reach the closed position, the dc motor is stopped, and the SMA actuator is actuated by heating the array of parallel SMA wires by applying an electrical current. At this position,

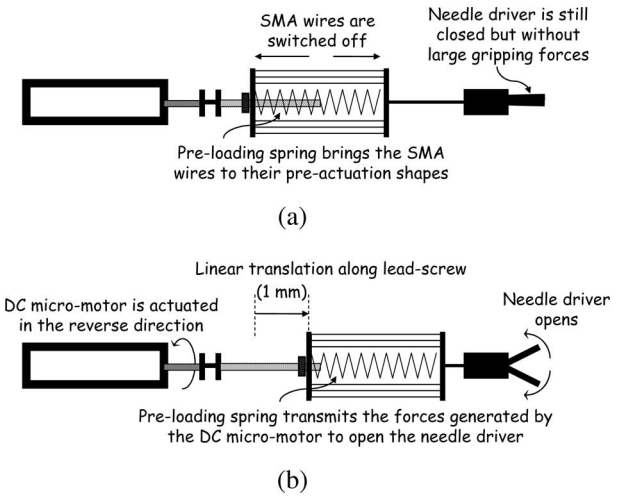

Fig. 2 Opening of the needle driver using the hybrid actuator. (a) SMA actuator is switched off followed by a short delay to allow the SMA wires to cool. (b) DC micromotor is then actuated to open the needle driver jaws. (The figures are not to scale.)

the force exerted by the needle driver jaws is at the peak value. The force generated by the SMA actuator is enough for the needle driver jaws to hold the needle for performing suturing. When the SMA actuator is activated, it does not backdrive the dc micromotor as the lead-screw nut assembly is not backdrivable because of the friction and pitch of the lead-screw.

B. Opening the Needle Driver Jaws

For opening the jaws of the needle driver (Fig. 2), the SMA actuator is switched off first. After the SMA actuator is cooled down, the dc motor is rotated in clockwise direction. The clockwise rotation of the screw causes the SMA actuator to move in the forward direction. Because of the short delay between the turning off of the SMA current and the starting of the dc micromotor to open the gripper, to allow for the cooling of the SMA, the SMA will not be applying a force when the dc micromotor is activated. Since the SMA wires cannot transmit the compressive forces, a preloaded spring is used to transmit the forces generated by the dc motor to open the needle driver jaws. As the motor continues to rotate, the needle driver jaws open up. The dc motor is switched off after the jaws open up.

IV. SMA Characteristics

In the construction of SMA stages of the actuator prototypes, we have used off-the-shelf 0.154-mm-diameter nickel–titanium SMA wires (Flexinol, Dynalloy, Inc., Costa Mesa, CA). However, the detailed force versus stroke length characteristics of the SMA wires, which is critical to determine the tolerances and the structural stiffness requirements of the mechanical design, were not available from the manufacturer. The following experimental setup and methodology was used to determine the characteristic curve. It has been included here as it may be of interest to the readers who need to determine similar characteristics for their own applications.

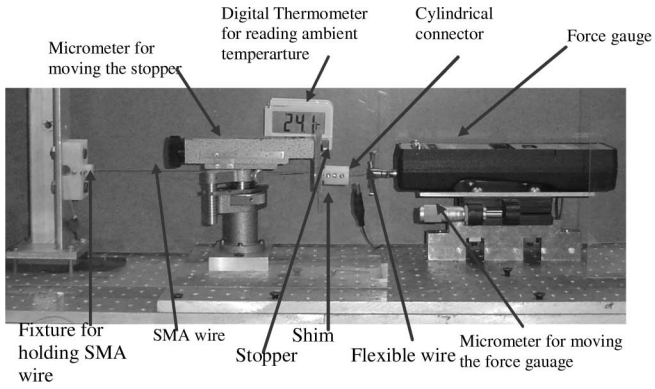

Fig. 3 Experimental setup for determining SMA characteristics.

The experimental setup shown in Fig. 3 is constructed to obtain the force versus stroke length characteristics of the SMA wire. One end of the SMA wire that will be characterized is connected to a fixture that is firmly fixed to a base plate, while the other end of the SMA wire is connected to a force gauge through a cylindrical connector and a flexible wire.[3] Initially, the force gauge is moved with the help of a micrometer in the direction that increases the tensile force in the SMA wire. As soon as the force gauge reading shows 0.5 N (to make the SMA wire taut), the movement is stopped, and the movable stopper is moved to transfer the load from the force gauge to the stopper. This is done by placing a shim in between the connector and the stopper, and moving the stopper toward the connector until the force gauge shows a reading of 0 N. Then, the SMA wire is actuated by passing current through it and heating it to 75–80 °C.[4] At this point, the SMA wire is actuated with both of its ends constrained, so the force generated in the SMA wire is approximately equal to the maximum force it can generate with zero strain. In order to measure this force value, the force gauge is slowly moved away from the stopper until the shim inserted in between the connector and the stopper falls, at which point the force gauge reading is approximately equal to the force generated in the SMA wire. The corresponding value of the micrometer reading is taken down. Once the initial reading is obtained for zero stroke length, the stopper is moved toward the fixture by a known displacement. Following this, the force gauge is moved toward the stopper, with the shim placed in between the connector and the stopper, until its reading becomes zero, transferring all the load back to the stopper. The force gauge is, then, again moved away from the stopper till the shim falls off. At this point, the reading on the gauge shows the force generated by the SMA wire for the displacement equal to the displacement of the stopper from its initial position. This process is then repeated for several displacement values of the stopper to obtain a set of force readings for the set of known stroke lengths.

[3]The stiffness of the supporting structure for holding the SMA fixture is measured before carrying the experiment, and is found to be very high for the forces applied during the experiment. Therefore, the supporting structure is treated as a rigid structure as the deformation at this end is negligible.

[4]The temperature of the SMA wire is measured using a temperature probe (FLUKE 80TK, Fluke Electronics, Everett, WA).

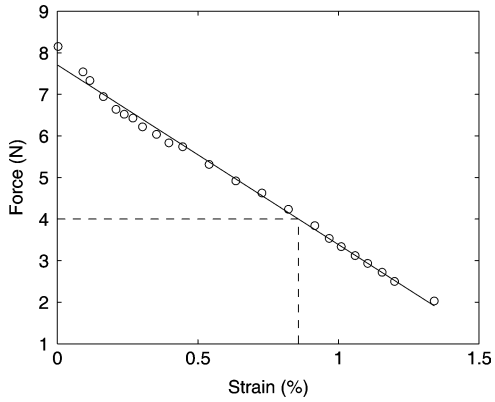

Fig. 4 Force versus stroke length characteristics of the SMA wire (0.154-mm-diameter wire).

We can determine the required structural stiffness and manufacturing tolerances of the actuator mechanism from Fig. 4. For example, the 0.154-mm-diameter SMA wire can generate a force of 4 N for a stroke strain of 0.8%. This means that an SMA actuator with eight SMA wires, each one 30 mm in length, connected mechanically in parallel can generate a minimum combined force of 32 N if the SMA actuator structure allows a maximum movement of approximately 0.25 mm from structural deformations and miscellaneous tolerances in the mechanism.

V. Design of the First-Generation Actuator Prototype

During the design of the first-generation hybrid actuator prototype, the main design objective was to minimize the overall dimensions of the actuator pack, while still satisfying the minimum force output requirements, at the expense of mechanism complexity.

As shown in Fig. 5, the millimeter-scale actuator prototype consists of a 3.4-mm-diameter and 12.22-mm-long brushless dc motor (Smoovy BL2S3.025.R.0, MPS Micro Precision Systems AG, Bienne, Switzerland) with a planetary gear reduction of 1:25. The 3.4-mm motor is connected to a 1.46-mm-diameter screw, with a pitch of 80 threads per inch, through a connector [Fig. 5(d)]. The connector acts as a bearing, and isolates the motor from any axial forces that are produced when the SMA actuator is actuated. The torque generated by the dc motor with 1:25 reduction gear train, as per the specifications provided in the data sheets, is 0.42 mN·m.

The SMA actuator consists of a 0.1524-mm-diameter SMA wire wound around the cylindrical Torlon (Solvay Advanced Polymers, LLC) structure through holes, as shown in Fig. 5(b). Torlon is used to fabricate the SMA actuator structure as it can withstand high temperatures, has good mechanical properties, and can be machined easily. This SMA wire acts as six individual SMA wires connected mechanically in parallel. The SMA actuator is preloaded with a spring to provide necessary reverse bias force to the SMA wire, as shown in Fig. 5(b). As the SMA wire cannot transmit compressive forces, the loaded spring transmits the compressive force required for opening of the gripper. The total length of the SMA wire used in the actuator is 150 mm, and the length of each individual wire connecting the SMA actuator is 25 mm.

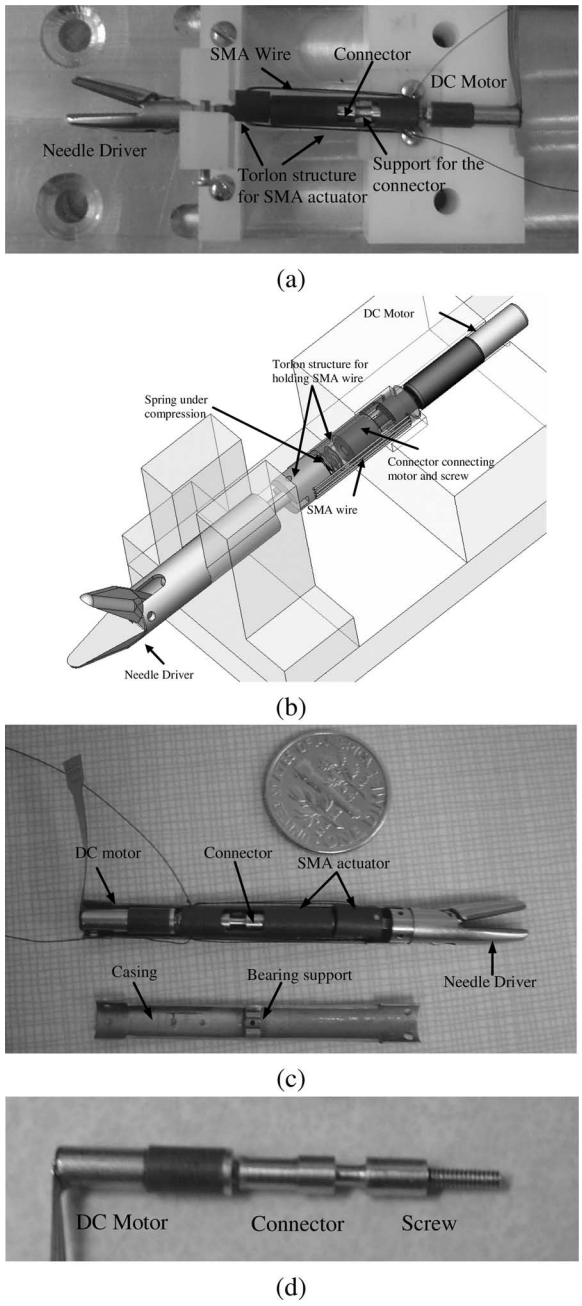

Fig. 5 First-generation design prototype. (a) Photograph of the prototype. (b) Computer-aided design (CAD) model of the design. (c) Assembly of the final design with casing. (d) Linear actuator consisting of dc motor, connector, and screw.

The designed prototype is interfaced to a computer through the printer port for controlling the motion of the gripper. The software code for generating the required signals is written in C++. The motor is controlled by a manufacturer controller (Smoovy BLCPS.000.2.8, MPS Micro Precision Systems AG, Bienne, Switzerland), and the required input signals for the controller are generated by the computer. The SMA actuator is controlled by switching an electromechanical relay ON and OFF

through the computer. First, the dc motor is actuated by giving a pulse signal to the input of the controller. Each pulse signal makes the dc motor rotate by 60°, and a total of 520 pulses are required to close/open the gripper. The total time taken by the dc motor to close the gripper is 1.5 s. The gripping force generated by this setup with a 10-mm-long needle driver jaw is 5.5 N, as measured at a distance of approximately 7.5 mm (three fourths of jaw length) from the gripper joint. This shows that the actual force generated by the SMA actuator is around 15 N, as there is a reduction in the force applied to the force exerted by the needle driver.

The first-generation actuator prototype is a rather compact design, as the linear displacement (i.e., dc micromotor stage) and the force-generation (i.e., SMA actuator) stages overlap partially. However, this design results in manufacturing and assembly issues, which result from the complicated moving parts. In particular, the performance of the linear stage is very sensitive to the alignment of the motor shaft and the connector, and therefore, results in machining and assembly difficulties. This can be overcome by using a flexible coupling between the motor shaft and the connector, which, however, significantly complicates the overall design at this scale. The second issue with the first-generation design concerns the casing of the actuator. As shown in Fig. 5(c), the casing for the hybrid actuator consists of a bearing support structure to hold the actuator assembly in place and protect the motor from axial forces. The casing is made of steel, as the thickness of the casing needs to be very thin, and it has to provide structural stability to the actuator assembly. The idea of Teflon coating on the inner side of the casing was pursued in order to electrically isolate the SMA wires from the casing. Given the tight tolerances of the parts, the Teflon coating can be only on the order of micrometer thickness. At this thickness, it is very difficult to control the density and uniformity of the Teflon coating resulting in a significant manufacturing challenge. Therefore, a second-generation hybrid actuator was designed to overcome these problems.

VI. Design of the Second-Generation Hybrid Actuator

The second-generation actuator is designed in such a way that the assembly of the various parts inside the actuator is simple, and all the parts can be assembled inside a 4.6-mm inner diameter casing. As shown in Fig. 6, the constructed final actuator is 5.14 mm in diameter and approximately 60 mm in length. The outer casing needs to be very thin and should provide structural support to the actuator assembly. The outer casing for the hybrid actuator is fabricated out of Celazol (Quadrant Engineering Plastic Products, Reading, PA), as Celazol has better mechanical properties when compared to Torlon in terms of tensile strength and operating temperature.

A. Design of the SMA Actuator Stage

The SMA actuator stage of the second-generation prototype, as shown in Fig. 7, consists of a lower fixture, an upper fixture, a spring holder, and a spring. The major and minor diameters of the lower fixture and upper fixture are 4.2 and 3.2 mm, respectively. Lower and upper fixtures for the SMA actuator are

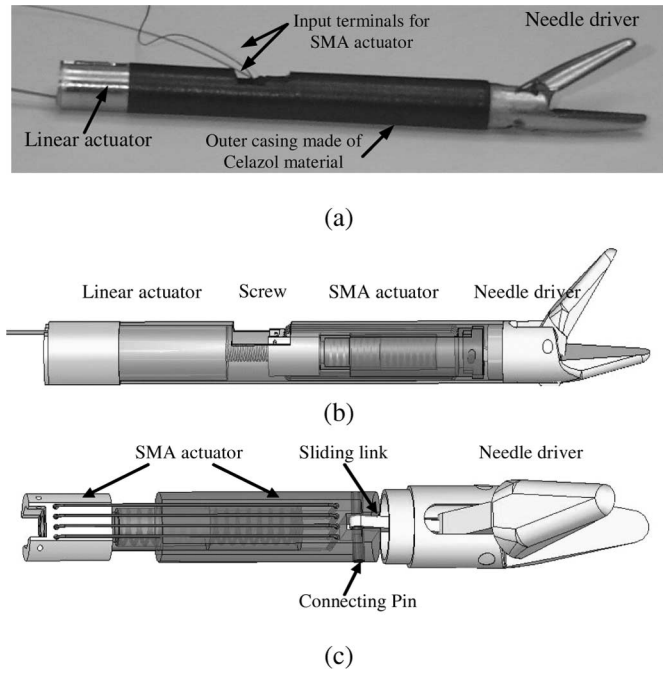

Fig. 6 Second-generation design prototype. (a) Photograph of the prototype. (b) CAD model of the design. (c) CAD model of the assembly of SMA actuator and the needle driver.

fabricated from Torlon material. Torlon was selected for fabricating the SMA actuator as it can withstand high temperatures, can be machined easily, and isolates the SMA wires electrically. The lower fixture contains 0.3-mm-diameter holes to hold the SMA wire and for tying a knot to secure the ends of the SMA actuator. The spring holder acts as a housing for the spring that is used to provide reverse bias force to the SMA wire. The end of the spring holder that goes into the lower fixture contains a threaded hole to move the SMA actuator linearly when the screw shaft on the linear actuator is rotated. The spring holder for the actuator is made of brass. The reason for using brass to fabricate the spring holder is that it acts as a heat sink for the SMA actuator, and provides low friction between the screw and the threaded hole. There is a clearance between the spring holder casing and the inner diameter of the upper fixture, so that the spring holder can slide inside the upper fixture. Upper fixture is also fabricated from Torlon, and it holds and connects the SMA actuator to the needle driver.

Fig. 7(b) shows an exploded view of the SMA actuator. During the assembly of the SMA actuator, the spring holder and the lower fixture are first joined together by applying instant adhesive. Then, the assembly of the spring holder and lower fixture is loaded into the upper fixture with the spring in between them. This assembly is loaded into the SMA weaving instrument for holding the components of the SMA actuator in position, under the compressive force of the loaded spring, as shown in Fig. 7(d). The SMA weaving instrument is made of Torlon material. In order to provide the reverse bias force on the SMA wire, the assembly of the lower fixture, spring holder, and the upper fixture are locked in a position by a positioning pin such that the spring is compressed in between the lower fixture and the upper fixture. Once the position of the assembly is secured in

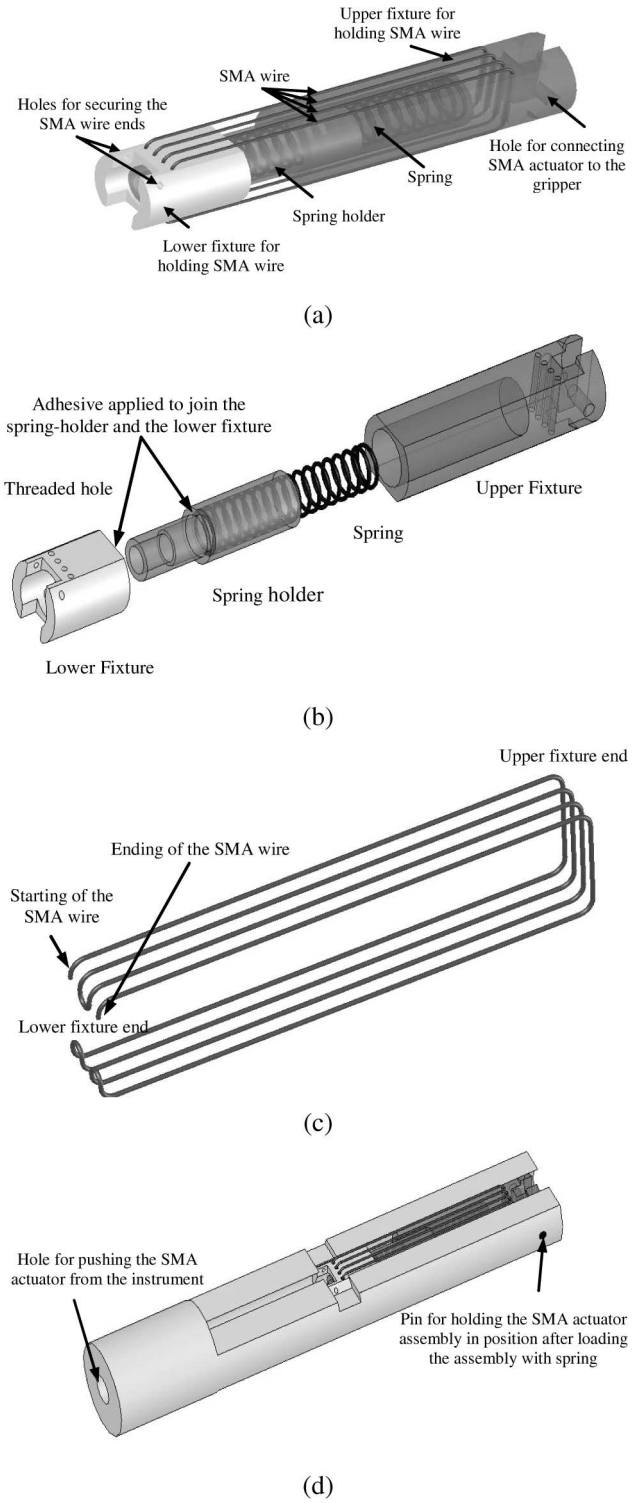

Fig. 7 Details of the SMA actuation stage of the second-generation design prototype. (a) CAD model of the SMA actuator stage. (b) Exploded view of the SMA actuator stage. (c) Weaving path of the SMA wire. (d) SMA weaving instrument.

the SMA weaving instrument, the SMA wire is weaved around the assembly, as shown in Fig. 7(c). The two ends of the SMA wire are secured to the lower fixture by tying a knot through the two additional holes provided on the lower fixture. Thermal resistive adhesive from Loctite (4211 PRISM, Henkel Corporation, Rocky Hill, CT) is applied on the knot to make sure that the SMA wire remains in position once the positioning pin is removed. Thermal resistive adhesive is used because the temperature of the SMA wire reaches approximately 80 °C during the operation of the SMA actuator. Once the adhesive is cured, the positioning pin is removed, and the SMA actuator is removed by pushing it from the bottom of the SMA weaving instrument with a long thin rod.

B. Design of the Linear Actuator Stage

The linear actuator stage of the hybrid actuator consists of a 1.4-mm-diameter screw with a pitch of 0.3175 mm that is rotated by a micromotor, as shown in Fig. 8(a). The micromotor used in this hybrid actuator is a 4-mm-outer-diameter motor (SBL04-0829PG18, Namiki Precision Jewel Company, Ltd., Tokyo, Japan) consisting of a 4-mm-diameter gearbox with a reduction ratio of 1:18. The reason for selecting the Namiki motor over the Smoovy motor used in the first-generation prototype is that the output speed and the amount of output torque generated by the Namiki motor are greater than that by the Smoovy motor. The total length of the motor is 18 mm including the length of the shaft. A hole of 0.8-mm diameter and 3-mm length is drilled into the end containing the head of the screw. The motor shaft is slid through this hole, and instant adhesive from Loctite (411 PRISM, Henkel Corporation, Rocky Hill, CT) is applied to hold the motor shaft and the screw.

As shown in Fig. 8(b), a key is attached to the casing of the motor. The screw and the motor assembly are slid into the motor holder such that the key on the motor casing is in between the key way of the motor holder. The key attached to the casing of the motor prevents the motor casing from rotating, but allows it to move linearly. The motor supporting structure is fixed to the end of the motor holder to fix the motor inside the motor holder. A small clearance is left in between the motor and the supporting structure so that the motor can slide by a fraction of a millimeter. The main advantage of this type of motor assembly is that the motor shaft is free from any high axial load that is generated during the operation of the SMA actuator, as the entire load is taken by the screw head.

C. Assembly Procedure

During the assembly, the SMA actuator is first attached to the sliding link of the needle driver, as shown in Fig. 6(c). A connecting pin is used to connect the sliding link and the SMA actuator. There is clearance provided in between the sliding link and the connecting pin, so that the connecting pin can freely pivot over the sliding link. There is a tight fit between the SMA upper fixture and the connecting pin; as a result, the connecting pin stays with the upper fixture of the SMA actuator.

After assembling the SMA actuator and needle driver, the casing is assembled by applying adhesive between the needle driver and the inner surface of the casing. Then, the linear actuator is connected to the drive circuit and is rotated in the anticlockwise direction. Rotation of the linear actuator in the clockwise direction makes the screw advance in the forward direction into the SMA actuator. Once the linear actuator is inside the outer

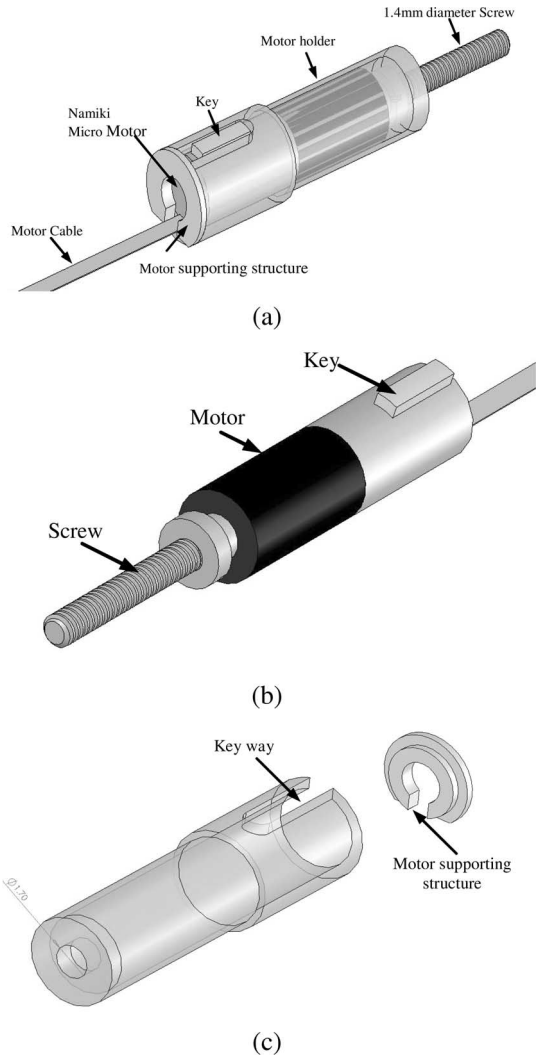

Fig. 8 Linear actuator stage of the second-generation design prototype. (a) CAD drawing of the linear actuation stage. (b) Motor and screw assembly. (c) Motor holder and supporting structure.

casing, adhesive is applied to attach the linear actuator to the casing firmly.

D. Experimental Results

A plot of the signals required for one complete cycle of the second-generation hybrid actuator is shown in Fig. 9. First, the dc motor is actuated by giving an input signal to the input of the Namiki motor drive unit (SSD04). Namiki motor drive drives the motor in open loop as the motor does not have any feedback sensors. The total time taken by the dc motor to close the gripper is 0.4 s (t_{close}). The direction of rotation of the dc motor depends on the direction signal. At the end of 0.4 s, after the gripper closes, the SMA actuator is actuated by switching an electromechanical relay switch ON. The SMA actuator is actuated while the gripper needs to hold the needle, for a time of t_{hold} seconds. The amount of gripping force applied on a needle located at approximately 7.5 mm (three-fourths of jaw length) from the gripper joint is 8 N. The dc motor is not actuated

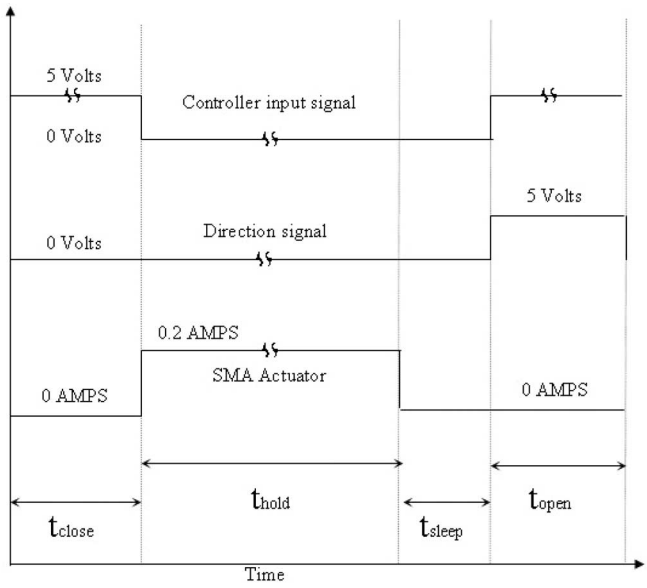

Fig. 9 Waveformplot for controlling the second-generation hybrid actuator. The SMA wire is actuated by 0.2 A of current provided from a current amplifier. Other signals are logic signals.

immediately after switching OFF the SMA actuator. It is rather actuated after a time delay of 1 s (t_{sleep}). The time delay is necessary to make sure that the SMA actuator has relaxed and is not applying a high axial force on the linear actuator. At the end of the t_{sleep} seconds, the dc motor is actuated to open the gripper jaws. The dc motor rotates in the clockwise direction as the direction signal changes from 0 to 5 V. The total time required for one complete cycle excluding the duration while holding the needle is 1.8 s. This cycle time includes the time t_{sleep} required for cooling down of the SMA. A video of the tests of the system is provided for view in [24].

VII. Discussion and Conclusion

This paper addressed the need for a local actuation system to actuate the end-effector of a robot performing MIS. We discussed a novel design idea for developing a hybrid actuator as a local actuation system. The force versus stroke length characteristics are determined for the SMA wire used in the design of the actuator. We developed a prototype to test the feasibility of the design idea, and tested it to determine the amount of gripping force generated. The resulting performance values for the two generations of hybrid actuator designs are summarized in Table III.

There is a large scope of improvements for this hybrid actuator to increase its performance. Presently, the actuator operates as a feedforward device without any position feedback. One improvement that can be done in this area is to use microposition sensors to get feedback of the absolute position of the end-effector opening angle. The amount of force required for holding the needle is different from the force required to hold the tissue. So, if microforce sensors can be embedded onto the needle driver jaws, the SMA actuator can be controlled to generate appropriate amount of force based on whether it has to

TABLE III
SUMMARY OF THE FINAL ACTUATOR DESIGN PARAMETERS

Parameter	First Generation Prototype Values	Second Generation Prototype Values
Dimension: overall diameter		
without casing	4.5mm	4.6mm
with casing	n/a	5.14mm
Dimension: overall length		
excluding needle driver	42mm	40mm
Actuator force	15N	24N
Gripping force	5.5N	8N
Actuator stroke length	1mm	1mm
Gripper opening angle	45^o	45^o
Gripper cycle time (including SMA cool-off delay)	4 sec	1.8 sec

hold the needle or the tissue. These two additions would allow a completely analog control of the hybrid actuator.

Presently, the outer casing of the actuator is fabricated from Celazol, which is an electrical and thermal insulator. This material was specifically chosen to provide the thermal and electrical insulation necessary for the safety of the end-effector. As a result, the performance of the actuator may be reduced if the SMA actuator is switched ON for long time, due to overheating of the internal parts of the actuator. In the current prototype, the heat is dissipated by convection. Because of the high thermal resistivity of the casing, we have not observed any significant temperatures at the surface of the actuator assembly. However, this may become an issue if a metallic casing is used, and therefore, needs to be considered if such a design will be employed. The heat generation by the SMA wire can be a safety concern for regulatory approval, especially for the case of a metallic casing. This can be handled by placing a temperature sensor inside the actuator unit. The improvement in SMA cooling efficiency would also help to decrease the cycle time of the actuator.

Another design possibility is to construct the outer casing using brass or surgical steel, coating the interior surface with a very thin layer (sufficiently thick to provide adequate electric insulation) of Teflon. Unlike the first-generation prototype, where Teflon coating of the interior of the casing was difficult because of the presence of a bearing, this is rather straightforward for the second-generation prototype as there is no bearing, or any other additional structures, present on the inner surface of the casing that would make coating difficult.

Maintaining reliable electrical connection with SMA wires is a common issue in SMA actuator applications. In the limited test that we have performed with our prototype, we have not observed any issues with knots; however, we have not performed extensive reliability tests for electrical connections. This is an issue that needs to be kept in mind for the application of the technology. Mechanical clamping or welding are two potential candidates for consideration if the proposed hybrid actuator is to be mass-produced. The welding of SMA typically results in change of shape memory properties locally, but it is not expected to effect performance of the proposed hybrid actuator as the location where the connection is made does not need to be carrying a load.

The present design uses a needle driver unit adapted from an off-the-shelf endoscopic needle driver instrument, and is not designed to give optimum performance for use with the hybrid actuator. If a custom gripper is designed for the hybrid actuator, it can decrease the overall length of the actuator and can increase the amount of force applied.

The overall outer diameter of the second-generation actuator, together with the casing, is slightly above the design specifications given in Table I. The main reason for this is the clearance required to attach the actuator outer casing to the off-the-shelf needle driver unit. If the needle driver was custom-built, together with the actuator outer casing, instead of adapting a needle driver unit from a commercial manual instrument, the outer diameter specification would be very easily satisfied. However, we chose not to pursue this option as this would have been a distraction from the actual research topic of the design of the hybrid actuator.

The required gripping force of the actuator is an important design variable, and depends on the needle driver jaw size and texture, the needle size and shape, and the type of tissue that the tissue will be driven into. Therefore, it might be necessary to have higher gripping forces for some applications (e.g., [25]). It is rather straightforward to increase the gripping force for the proposed design of the hybrid actuator by increasing the number or diameters of the SMA wires used. However, it is important to note that using SMA wires of larger diameters will lead to longer cool-off times.

The cost of the developed prototype is an important concern for the feasibility of a commercial product using the design. Costs of the micromotors and sensors at this scale are likely to decrease, especially as production numbers escalate. For example, micromotors with slightly larger sizes are commercially available for about US $0.50, since they are widely used as vibrators in cell phones.

The goal of the proposed end-effector design is to enable the development of 6-DOF surgical manipulators with spherical wrists and tool shaft diameters of 5 mm, which has not been possible in any commercial or research systems developed so far (see Section I). We believe this is the value added of the proposed design, and may or may not justify the increased cost and complexity from using the proposed end-effector based on the application. Furthermore, the premise of the proposed design is that routing of electrical cables through a wrist to power the local actuator would be smaller, easier, and cheaper than is designing a system where mechanical power is routed through the wrist, which may not even be possible for a 5-mm-diameter wrist.

The present research work was only focused on the design of the local actuation system, and did not look into the design of a spherical wrist for minimally invasive robotic surgery (MIRS) applications. Future research work will proceed toward the design of a spherical wrist that employs the developed locally actuated end-effector design.

ACKNOWLEDGMENT

The authors would like to thank Prof. W. Newman for his suggestions during this work, especially for the SMA characterization.

REFERENCES

[1] L. W. Way, S. Bhoyrul, and T. Mori, Eds., *Fundamentals of Laparoscopic Surgery*. New York: Churchill Livingstone, 1995.

[2] R. H. Taylor and D. Stoianovici, "Medical robotics in computer integrated surgery," *IEEE Trans. Robot. Autom.*, vol. 19, no. 5, pp. 765–781, Oct. 2003.

[3] M. Goldfarb and N. Celanovic, "A flexure-based gripper for small-scale manipulation," *Robotica*, vol. 17, no. 2, pp. 181–188, 1999.

[4] S. Kota, K.-J. Lu, Z. Kreiner, B. Trease, J. Arenas, and J. Geiger. (2005). Design and application of compliant mechanisms for surgical tools. *J. Biomech. Eng.* [Online] *127(6)*, pp. 981–989. Available: http://link.aip.org/link/?JBY/127/981/1.

[5] G. Tholey, A. Pillarisetti, W. Green, and J. P. Desai, "Design, development, and testing of an automated laparoscopic grasper with 3-d force measurement capability," in *Proc. Med. Simul.: Int. Symp. (ISMS 2004)*, pp. 38–48.

[6] D.-H. Kim, M. G. Lee, B. Kim, and Y. Sun, "A superelastic alloy microgripper with embedded electromagnetic actuators and piezoelectric force sensors: A numerical and experimental study," *Smart Mater. Struct.*, vol. 14, pp. 1265–1272, 2005.

[7] K. Koehn and S. Payandeh, "Toward evaluation of shape memory alloy actuators for endosurgery," in *Proc. IEEE Int. Conf. Syst., Man, Cybern.*, 1995, vol. 3, pp. 22–25.

[8] I. Karjalainen, T. Sandelin, R. Heikkilä, and R. Tuokko, "Using piezoelectric technology to improve servo gripper performance in mini- and microassembly," *Assem. Autom.*, vol. 25, no. 2, pp. 117–123, Jun. 2005.

[9] Z. W. Zhong and C. K. Yeong, "Development of a gripper using SMA wire," *Sens. Actuators A*, vol. 126, pp. 375–381, 2006.

[10] M. C. Çavuşoğlu, F. Tendick, M. Cohn, and S. S. Sastry, "A laparoscopic telesurgical workstation," *IEEE Trans. Robot. Autom.*, vol. 15, no. 4, pp. 728–739, Aug. 1999.

[11] A. J. Madhani, "Design of teleoperated surgical instruments for minimally invasive surgery," Ph.D. dissertation, Massachusetts Inst. Technol., Cambridge, MA, 1998.

[12] S. Bobbio, M. Kellam, B. Dudley, S. G. Johansson, S. Jones, J. Jacobson, F. Tranjan, and T. DuBois, "Integrated force arrays," in *Proc. IEEE Micro Electro Mech. Syst. Workshop*, Fort Lauderdale, FL, Feb. 1993, pp. 149–154.

[13] S. Park and T. Shrout, "Ultrahigh strain and piezoelectric behavior in relaxor based ferroelectric single crystals," *J. Appl. Phys.*, vol. 82, pp. 1804–1811, 1997.

[14] I. Hunter, S. Lafontaine, J. Hollerbach, and P. Hunter, "Fast reversible NiTi fibers for use in microrobotics," in *Proc. 1991 IEEE Micro Electro Mech. Syst. (MEMS'91)*, pp. 166–170.

[15] H. Tobushi, S. Hayashi, and S. Kojima, "Mechanical properties of shape memory polymer of polyurethane series," *JSME Int. J., Ser. I*, vol. 35, no. 3, pp. 296–302, 1992.

[16] S. Canfield, B. Edinger, M. Frecker, and G. Koopmann, "Design of piezoelectric inchworm actuator and compliant end-effector for minimally invasive surgery," in *Proc. SPIE 6th Int. Symp. Smart Mater. Struct.*, Newport Beach, CA, 2003, pp. 3668–3678.

[17] D. Grant and V. Hayward, "Constrained force control of shape memory alloy actuator," in *Proc. IEEE Int. Conf. Robot. Autom.*, San Francisco, CA, 2000, pp. 1314–1320.

[18] S. Hirose, K. Ikuta, and M. Tsukamoto, "Development of a shape memory alloy actuator. Measurement of material characteristics and development of active endoscopes," *Adv. Robot.*, vol. 4, no. 1, pp. 3–27, 1995.

[19] M. Shahinpoor and G. Wang, "Design and modelling of a novel fibrous shape memory alloy (SMA) actuator," in *Proc. SPIE, Smart Struct. Mater. 1994: Smart Struct. Intell. Syst.*, vol. 2190, pp. 730–738.

[20] R. Kornbluh, R. Pelrine, J. Eckerle, and J. Joseph, "Electrostrictive polymer artificial muscle actuators," in *Proc. IEEE Int. Conf. Robot. Autom. (ICRA 1998)*, pp. 2147–2154.

[21] J. Peirs, D. Reynaerts, and H. V. Brussel, "Design of miniature manipluators for integration in self-propelling endoscope," in *Proc. Actuator 2000, 7th Int. Conf. New Actuators*, pp. 603–606.

[22] M. V. Ottermo, O. Stavdahl, and T. A. Johansen, "Electromechanical design of a miniature tactile shape display for minimally invasive surgery," in *Proc. 1st Joint Eurohaptics Conf. Symp. Haptic Interfaces Virtual Environ., Teleoperator Syst. (WHC 2005)*, pp. 561–562.

[23] M. V. Ottermo, O. Stavdahl, and T. A. Johansen, "Palpation instrument for augmented minimally invasive surgery," in *Proc. 2004 IEEE/RSJ Int. Conf. Intell. Robots Syst.*, pp. 3960–3964.

[24] V. R. Kode and M. C. Çavuşoğlu (2006). Millirobotic tools for minimal invasive surgery: Video of hybrid gripper tests, [Online]. Available: http://robotics.case.edu/research.html\#medicalrobotics.

[25] A. J. Madhani, G. Niemeyer, and J. K. Salisbury, "The black falcon: A teleoperated surgical instrument for minimally invasive surgery," in *Proc. IEEE/RSJ Int. Conf. Intell. Robots Syst. (IROS 1998)*, vol. 2, pp. 936–944.

Venkata Raghavaiah Chowdhary Kode received the B.Tech. degree in mechatronics engineering from Mahatma Gandhi Institute of Technology, Hyderabad, India, in 2002, and the M.S. degree in electrical engineering from Case Western Reserve University, Cleveland, OH, in 2005.

He is currently a Mechatronics Design Engineer with Visicon Inspection Technologies, Napa, CA. His current research interests include robotics, human–machine interfaces, and design of medical tools for minimally invasive surgery.

M. Cenk Çavuşoğlu (S'93–M'01–SM'06) received the B.S. degree in electrical and electronic engineering from Middle East Technical University, Ankara, Turkey, in 1995, and the M.S. and Ph.D. degrees in electrical engineering and computer sciences from the University of California, Berkeley, in 1997 and 2000, respectively.

From 2000 to 2002, he was a Postdoctoral Researcher and Lecturer in the Department of Electrical Engineering and Computer Sciences, University of California, Berkeley. He is currently an Assistant Professor of electrical engineering and computer science at Case Western Reserve University, Cleveland, OH. His current research interests include robotics (medical robotics and haptics), virtual environments and computer graphics (surgical simulation and physical modeling), and systems and control theory.

Dr. Çavuşoğlus is an Associate Editor of the IEEE TRANSACTIONS ON ROBOTICS.